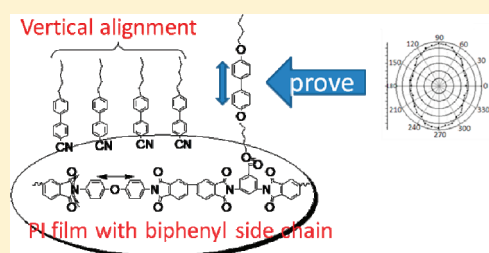


# Characterization of Alignment Correlation between LC Molecules and Chemical Groups on/in the Surface of Polyimide Films with Biphenyl Side Chains

Xu Wang, Peng Zhang, Yi Chen, Longbo Luo, Yuwei Pang, and Xiangyang Liu\*

State Key Laboratory of Polymeric Materials Engineering, College of Polymer Science and Engineering, Sichuan University, Chengdu 610065, P.R. China

**ABSTRACT:** In this study, the surface chemical structure and molecular conformation of one kind of PI alignment film achieving vertical alignment were investigated by XPS, ATR-FTIR, and polarized ATR-FTIR, and the LC alignment on PI film was studied by transmission polarized FTIR. It was found that some chemical groups, such as biphenyl and imide ring, oriented perpendicular to the plane of alignment film while the molecular backbones took the conformation parallel to the plane of film. At the same time, the biphenyl groups of LC molecules in LC cell were aligned perpendicular to the alignment film. Thus, the alignment consistency between the biphenyl in the surface and LC molecules was proved first, which powerfully indicated that the chemical groups in the surface taking a vertical conformation on the surface play an essential role in producing a vertical LC alignment and the conformation of groups in the surface determines the size of pretilt angle.



## 1. INTRODUCTION

In recent years, due to poor processability, low pretilt angle, and low transmittance in the visible region, the conventional aromatic polyimides hardly satisfy the requirements of manufacturing liquid crystal display (LCD) with high performance.<sup>1,2</sup> These disadvantages could be overcome by modifying the chemical structures such as introducing side chain groups,<sup>3–6</sup> fluorinated groups,<sup>7,8</sup> and a twisted structure<sup>9</sup> or replacing aromatic groups with alicyclic groups.<sup>10–13</sup>

To provide the theoretical basis for getting the most effective approach improving the alignment properties, it is necessary to elucidate the mechanism that controls LC pretilt angle on polyimide alignment. It is considered that the surface chemical structure and conformation of polyimides exerts an important effect on pretilt angle of LC cells.<sup>14–16</sup> Mi Hye Yi reported that the pretilt angles were affected by a geometric structure of side chain on the PI film surface.<sup>14</sup> K. Sakamoto considered that a pretilt angle of LC molecules is mainly affected by van der Waals interactions and the inclination angle of polymer backbones.<sup>15</sup> Yaw-Terng Chern investigated the effect of the configuration of the PI alignment layer on the pretilt angle and confirmed that the PI alignment films that contain out-of-plane units can generate high pretilt angles.<sup>16</sup> However, it has not been proved whether there exist the alignment consistence between LC molecules and chemical units on the surface of PI alignment film. There are still some people considering that the conformation of chemical group in the alignment film has an important role in determining the pretilt angle of LC molecules on the film,<sup>14,17</sup> which caused us to realize the necessity of studying the effect of alignment film surface on alignment of LC molecules.

To further understand the effect of alignment film surface on alignment of LC molecules, it is necessary to elucidate the alignment of units on the surface and to discover the alignment correlation between LC molecules and chemical groups of polyimide films on the surface. In this study, we designed one kind of PI alignment film with side chains containing a rigid biphenyl group based on biphenyltetracarboxylic dianhydride (BPDA), 4,4'-oxydianiline (ODA), and 4'-butoxy-4-(3,5-diaminobenzoyloxy)hexyloxybiphenyl (C6BBC4). The pretilt angle of LC molecules on this alignment film can run up to 90°, which only indicates that the LC molecules orient perpendicular to the plane of alignment film. However, it is unclear how the biphenyl side chains of PI alignment films orient. Thus, the chemical structure and molecular configuration on the film surface were investigated by XPS, ATR-FTIR, and polarized ATR-FTIR. In particular, it was investigated whether the para-direction of the biphenyl group in LC molecule oriented perpendicular to the alignment film for the vertical aligned LC cell. This may provide a new way to further investigate the alignment mechanism of achieving every pretilt angle for PI films.

## 2. EXPERIMENTAL SECTION

**2.1. Polymerization and Film Preparation.** The poly(amic acid)s were polymerized from C6BBC4 (synthesized by our group) with different ratios of ODA and BPDA. The polymerization procedure was given below. To a 25 mL three-necked round-bottom flask equipped with a mechanical

**Received:** August 3, 2011

**Revised:** October 9, 2011

**Published:** November 29, 2011

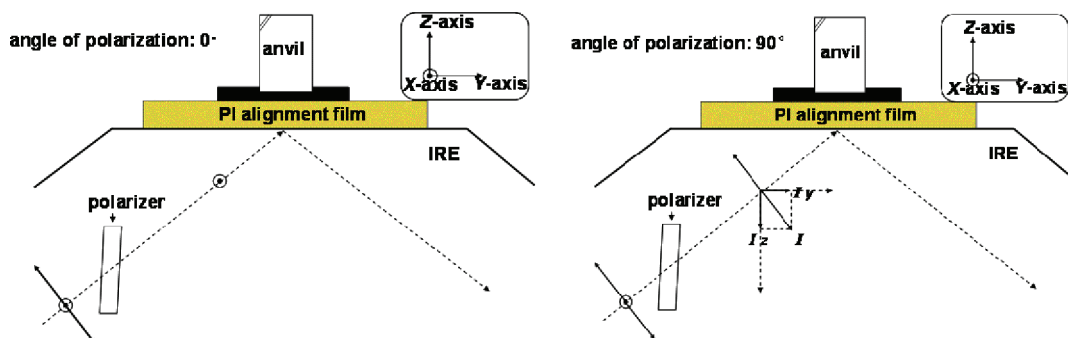


Figure 1. Scheme of ATR-FTIR: left, 0° polarized angle; right, 90° polarized angle.

stirrer and a nitrogen-inlet, C6BBC4 and ODA (total molar amount 0.001 mol) were dissolved in NMP, and then BPDA (0.3001 g, 0.0012 mol) was added into the solution. The reaction mixture was stirred at 0 °C for 12 h with a nitrogen flow to give a yellow poly(amic acid) solution. The solid content of the solutions were 10 wt %. The molar content of C6BBC4 was controlled to 0%, 30%, 60%, 85%. The PIs from the corresponding poly(amic acid)s were named as PI-0, PI-30, PI-60, and PI-85, respectively.

For measuring pretilt angles, poly(amic acid) solutions were spin-coated on 25 × 25 mm ITO-coated glasses at 500 rpm for 5 s and 1500 rpm for 10 s, respectively, followed by thermal imidization under 230 °C for 1 h. These films were used for pretilt angle, XPS and ATR-FTIR measurement. The films coated on CaF glass plates were used for polarized FTIR measurement of LC cell.

**2.2. LC Cell Fabrication and Pretilt Angle Measurement.** The prepared PI films on the ITO-coated glass or CaF glass were subsequently rubbed with a roller covered commercial rubbing cloth, and the rubbing strength  $L$  was calculated as follows:  $L = \ln(2\pi r n / 60v - 1)$ , where  $L$  (mm) was the total length of the rubbing cloth that touched a certain point of the film;  $l$  (0.3 mm) was the contact length of the rubbing roller circumference;  $N$  was the cumulative number of rubbings;  $v$  (17.2 mm/s) was the velocity of the substrate stage;  $n$  (700 rpm) and  $r$  (22.5 mm) were the rubbing roller speed and radius, respectively. LC cells were fabricated from two pieces of rubbed PI films assembled in an antiparallel rubbing direction with 43 μm (cell gap) thick spacers and filled with 4-pentyl-4'-cyanobiphenyl (5CB) by the capillary method. The pretilt angles for the fabricated LC cells were measured by a crystal rotation method with a PAT-20 measurement device (Chanchun Liancheng Instrument Co., Ltd.). Large pretilt angles near 90° were confirmed by conoscopy using a polarizing light microscopy (LEICA DMLP, Germany).

**2.3. Polarized FTIR Measurement of LC Molecules In LC Cell.** LC cells were fabricated from two pieces of PI films coated on CaF glass and filled with 5CB by the capillary method. These LC cells were directly measured by polarized FTIR with empty LC cells as background. Polarized FT-IR spectra were recorded on a Nicolet 560 Fourier transform spectrometer with variable polarization directions. Moreover, the pertilt angles of LC cells made of PI films on CaF glass was identical with that on ITO glass.

**2.4. Characterization.** ATR-FTIR and polarized ATR-FTIR spectra were recorded on a Nicolet 560 Fourier transform spectrometer using PI films coated on calcium fluoride glass. For polarized ATR-FTIR measurement, the polarized angle varied from 0° to 180° and a series of spectra were record by every 10 deg. XPS measurements were made with a Kratos ASAM 800 spectrometer (Kratos Analytical Ltd., Manchester, U.K.) using AlKα (1486.6 eV) monochromatized radiation. High resolution spectra were acquired with pass energy of 10 eV and a takeoff angle of 20° or 70°, respectively. The wedge cell for the measurement of the deviation angle was assembled with the top and bottom ITO glass rubbed in parallel directions with respect to each other. LC molecules

(5CB) were filled in the wedge cells. The anchoring energy was calculated by using the torque balance method, as shown in the refs 18 and 19.

The pretilt angle of LC cell fabricated from PI-85 without rubbing process was 90°. The pretilt angle of LC cell fabricated from rubbed PI-85 was 89°, and the anchoring energy of the PI-85 film with 60 rubbing strength was  $9.78 \times 10^{-5}$  N/m.

### 3. THEORETICAL BASIS

A schematic figure for the polarized ATR/FT-IR spectroscopy is shown in the Figure 1. A PI film is positioned onto the surface of the prism, with an internal reflection element (IRE), made of highly refractive materials (ZnSe) used to realize total reflection of the incident light. The angle of incidence of the ZnSe IRE is 45°. Polarized ATR-FTIR spectra were obtained using polarized IR radiation with different electric vector. Angle of polarization ( $\theta$ ) corresponds to the angle between electric vector of incident light and X-axis direction. The intensity of incident light is a constant  $I$ . Axial components ( $I_X$ ,  $I_Y$ ,  $I_Z$ ) are up to the angle of polarization ( $\theta$ ) of incident light and can be defined as eq 1, 2 and 3.<sup>20,21</sup>

$$I_X = \cos \theta \times I \quad (1)$$

$$I_Y = \sin \theta \times I \times \sin 45 = \sqrt{2}/2 \times I \times \sin \theta \quad (2)$$

$$I_Z = \sin \theta \times I \times \cos 45 = \sqrt{2}/2 \times I \times \sin \theta \quad (3)$$

The  $A_\theta$  spectrum was obtained by polarized incident light with different angle of polarization. For example, the  $A_0$  spectrum was obtained by rotating the IR polarizer such that the electric vector of the incident IR beam was parallel to X-axis direction, angle of polarization 0° (Figure 1a);  $A_{90}$  spectrum was obtained with the electric vector perpendicular to X-axis direction, angle of polarization 90° (Figure 1b).

The dichroic ratio,  $R_{ATR}$ , is defined as eq 4.

$$R_{ATR} = \frac{A_0}{A_{90}} = \frac{H_{0^\circ}}{H_{90^\circ}} \quad (4)$$

### 4. RESULTS AND DISCUSSION

**4.1. XPS Analysis.** The primary analysis of the chemical elements and groups in alignment film surface with XPS was reported in this section. The XPS spectra of PI-BBC4–30 and PI-BBC4–85 were obtained with a takeoff angle 20° or 70°, which were shown in the Figure 1. The peak A at 288 eV are

assigned to the C atoms linked to O atom in ester bonds and imide rings.<sup>22,23</sup> The area of this peak ( $S_A$ ) can be used to represent the amount of molecular backbone in the surface. The

**Table 1.** Ratios of Peak A in Spectra of Different PI Film with Different Take-Off Angle

	PI film = PI-C6BBC4-30		PI film = PI-C6BBC4-85	
take-off angle, deg	70	20	70	20
$P_A$	0.083	0.062	0.061	0.036

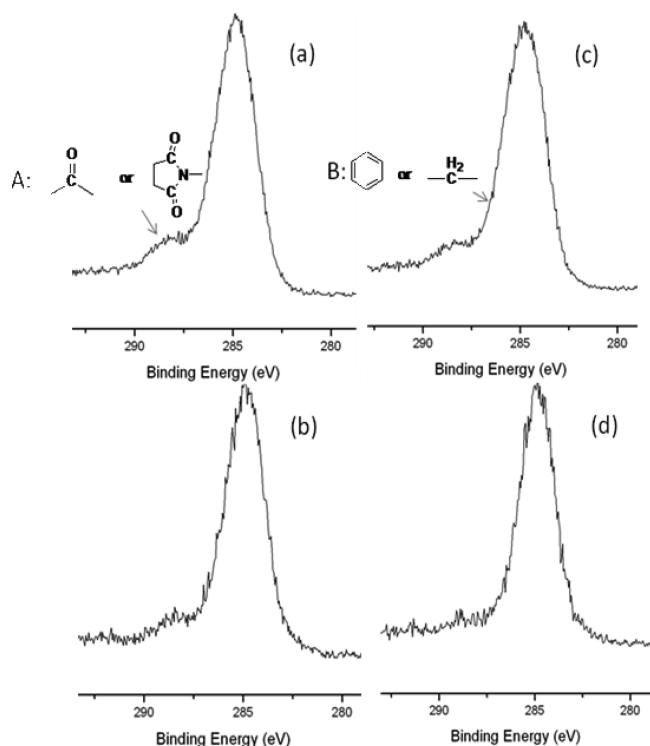


**Figure 2.** The C-XPS spectrum of different side chain content PI films under different takeoff angle: picture (a) PI-C6BBC4-30, takeoff angle 70°; (b) PI-C6BBC4-30, takeoff angle 20°; (c) PI-C6BBC4-85, takeoff angle 70°; (d) PI-C6BBC4-85, takeoff angle 20°.

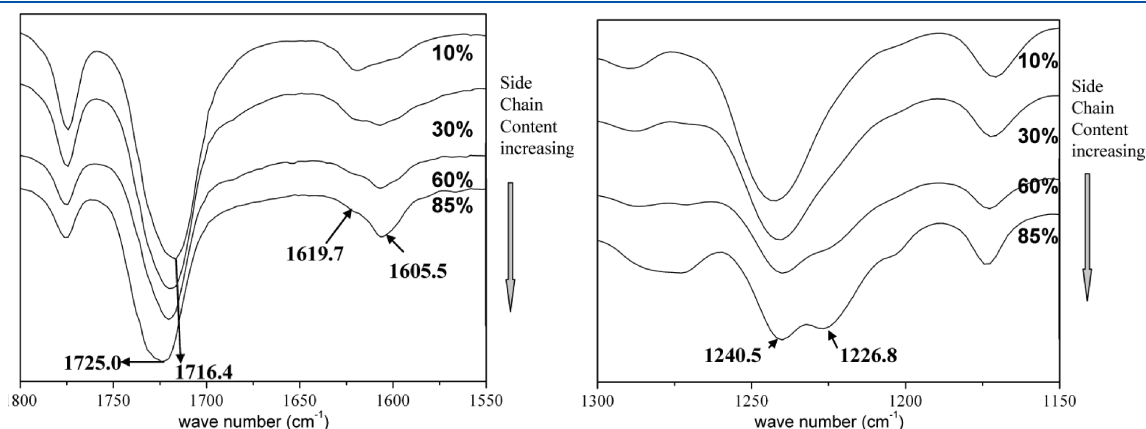


**Figure 3.** FTIR spectra of PI-C6BBC4 films with different content of side chain.

peak B at 285 eV corresponds to the C atoms in the alkyl chains and phenyl rings.<sup>22,23</sup> The ratio of main chain in the surface can be reflected by the proportion of peak A ( $P_A$ ), which is shown in the Table 1. The proportion of peak A was defined by eq 5.

$$P_A = S_A / (S_A + S_B) \quad (5)$$

As shown in the Figure 2 and Table 1, the proportion of peak A in spectra change clearly. The values of  $P_A$  of PI-C6BBC4-30 at 288 eV are obviously larger than that of PI-C6BBC4-85, which indicates that there are more side chains in PI-C6BBC4-85 film surface than in PI-C6BBC4-30 film surface. This results from the different side chain contents of two kinds of PI molecule.

However, for one kind of PI film, there still exists significantly difference in the  $P_A$  of the XPS spectrum with different take-off angle, 20° or 70°. The  $P_A$  of PI-C6BBC4-30 with a take-off angle of 20° is 0.062, less than 0.083 in spectrum with a take-off angle of 70°. For PI-C6BBC4-85, the  $P_A$  0.036 in the spectrum with a take-off angle 20° also is much less than 0.061 in the spectrum with a take-off angle of 70°. It can be indicated that the proportion of side chains in the surface of alignment film is obviously higher than that in the bulk, which is considered as the "enrichment" of side chain on the surface.

**4.2. ATR-FTIR Analysis.** These above results shown that side chain content in PI-C6BBC4-85 film surface is higher than that in the PI-C6BBC4-30 film surface, and the pretilt angle of LC molecules on PI-C6BBC4-85 film is much higher than that on PI-C6BBC4-30 film. According to other literatures, there are some dependences of pretilt angle on the side chain content and configuration on some PI films surface. For this kind of PI with side chain contain rigid biphenyl, there are very few details studies on the effect of polyimide molecular configurations on pretilt angle.<sup>24,25</sup> In order to characterize the alignment correlation between LC molecules and biphenyl side chains of polyimide films, the surface molecular structure sensitive technique of polarized ATR-FTIR was used to study the molecular configuration of side chained PI molecules on the film surface. Before analysis of polarized ATR-FTIR dates, it is necessary to complete infrared spectral assignments for this side-chained PI by comparing ATR-FTIR spectra of PI-C6BBC4 with different side chain content.

The ATR-FTIR spectra of PI films are shown in the Figure 3. According to the literature reports, these Peaks at about 1720  $\text{cm}^{-1}$ , 1610 and 1230  $\text{cm}^{-1}$  were assigned to C=O

asymmetric stretching vibration, 1,4-disubstituted, C–C stretching vibration and C–O–C stretching vibration, respectively.<sup>26,27</sup>

**Table 2.** Peak Positions of Kinds of Vibration of PI–C6BBC4 (Bands Assignment)

mode		wave number (cm <sup>-1</sup> )
$\nu(\text{C–O–C})_S$	C–O–C stretching vibration of side chain	1240.5
$\nu(\text{C–O–C})_B$	C–O–C stretching vibration of backbone	1226.8
$\nu(\text{C=O})_S$	C=O asymmetric stretching vibration of ester bond	1729.0
$\nu(\text{C=O})_B$	C=O asymmetric stretching vibration of imide ring	1716.5
$\nu(\text{C–C})_S$	C–C stretching vibration of 1,4-C <sub>6</sub> H <sub>4</sub> in side chain	1605.5
$\nu(\text{C–C})_B$	C–C stretching vibration of 1,4-C <sub>6</sub> H <sub>4</sub> in backbone	1619.7

With increasing side chain content, band spaces and intensities changed regularly. For example, two novel peaks appeared at 1605.5 and 1226.8 cm<sup>-1</sup> and increased clearly following the increase of side chain content, while peaks at 1619.7 and 1240.5 cm<sup>-1</sup> decreased obviously; the absorbance of C=O asymmetric stretching vibration at about 1720 cm<sup>-1</sup> was broadened and shifted to blue rang.

The increase of side chain content means that the concentration of side chained diamine (C6BBC4) increases, and the amount of ODA decreases accordingly in the procession of polymerization. It can be seen that the increase of C6BBC4 content resulted in increasing of peaks at 1605.5 and 1226.8 cm<sup>-1</sup>, and the decrease of ODA content resulted in decreasing of peaks at 1619.7 and 1240.5 cm<sup>-1</sup>. Thus, these two peaks at 1619.7 and 1605.5 cm<sup>-1</sup> were assigned to 1,4-disubstituted C–C stretching vibration of backbone and 1,4-disubstituted C–C stretching vibration of side chain, respectively. Absorption peaks of C–O–C stretching vibration of side chain and C–O–C stretching vibration of backbone appeared at 1226.8 and 1240.5 cm<sup>-1</sup>, respectively. There are two kinds of C=O asymmetric stretching vibration, ester bond in side chain and imide ring in molecular backbone. The blue shift of band at about

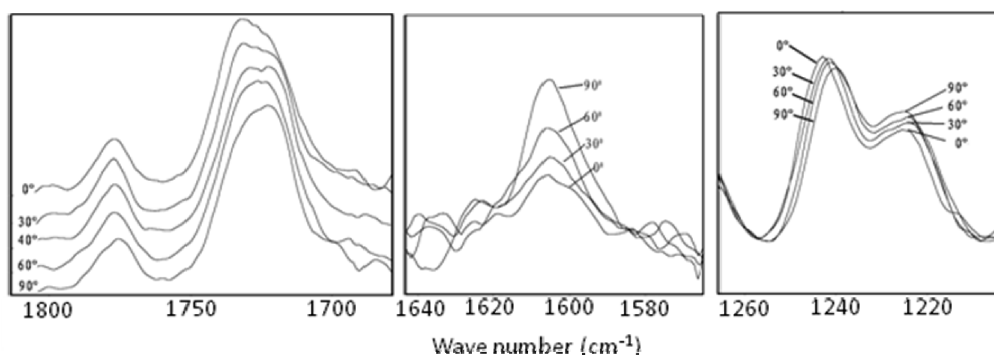


**Figure 4.** Peaks of FTIR spectra under different polarized angle.

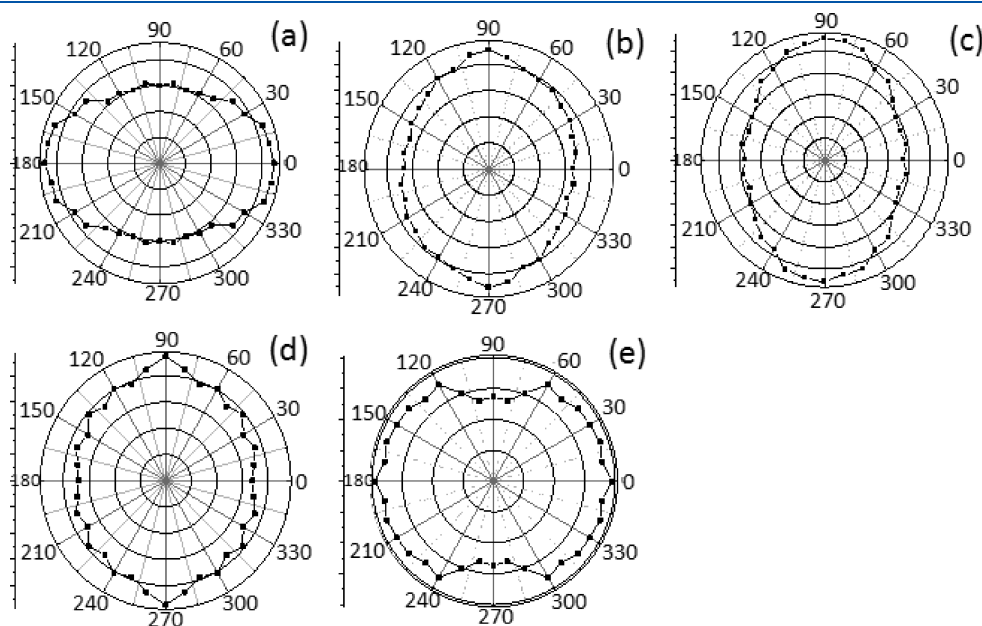


**Figure 5.** Polar diagrams of absorbance of peaks at different positions as a function of the angle of polarization of incident polarized light, obtained using linearly polarized IR spectroscopy: (a) 1729.0, (b) 1716.5, (c) 1605.5, (d) 1226.8, and (e) 1240.5 cm<sup>-1</sup>.



1720  $\text{cm}^{-1}$  indicates that the  $\nu(\text{C}=\text{O})$  absorption of ester bond occurs at a higher wavenumber comparing with that of imide ring. According to the following polarized ATR-FTIR spectra, absorption band of  $\nu(\text{C}=\text{O})$  split into two new peaks, respectively at 1716.5 and 1729.0  $\text{cm}^{-1}$ , which were assigned to  $\nu(\text{C}=\text{O})_{\text{S}}$  and  $\nu(\text{C}=\text{O})_{\text{B}}$ . Infrared spectral assignments for these valence-bone vibrations in molecular side chain and backbone are shown in the Table 2.

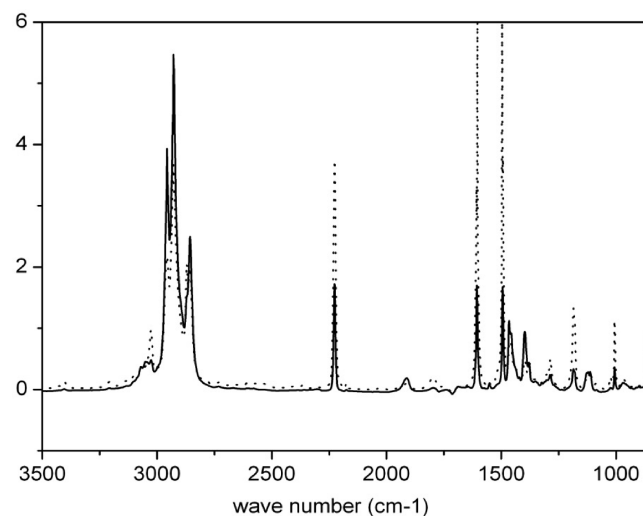
**4.3. Polarized ATR-FTIR Analysis.** The polarized ATR-FTIR spectra are shown in the Figure 4. It can be seen that the peak shapes and intensities at about 1720, 1610, and 1230  $\text{cm}^{-1}$  changed regularly with increasing of polarization angle from  $0^\circ$  to  $90^\circ$ . For example, the intensities of peaks at 1605.5 ( $\nu(\text{C}-\text{C})_{\text{S}}$ ) and 1226.8  $\text{cm}^{-1}$  ( $\nu(\text{C}-\text{O}-\text{C})_{\text{S}}$ ) increased clearly while peaks at 1619.7 ( $\nu(\text{C}-\text{C})_{\text{B}}$ ) and 1240.5  $\text{cm}^{-1}$  ( $\nu(\text{C}-\text{O}-\text{C})_{\text{B}}$ ) decreased obviously. Comparing with that in ATR-FTIR spectra, the absorption bands of  $\nu(\text{C}=\text{O})$  split into two new peaks in polarized ATR-FTIR spectra, and the peak at 1716.5  $\text{cm}^{-1}$  ( $\nu(\text{C}=\text{O})_{\text{B}}$ ) increased with increasing of polarization angle while the intensity of peak at 1729.0  $\text{cm}^{-1}$  ( $\nu(\text{C}=\text{O})_{\text{S}}$ ) decreased.

Figure 5 shows polar diagrams of absorbance of peaks at different positions as a function of the angle of polarization of incident polarized light, obtained using linearly polarized IR

**Table 3. Position and Dichroic Ratios for the Bands in the Spectra under Different Polarized Angle of Incident IR Beam**

positions ( $\text{cm}^{-1}$ )	$R_{\text{ATR}}$
1729.0 ( $\nu(\text{C}=\text{O})_{\text{S}}$ )	1.49
1716.5 ( $\nu(\text{C}=\text{O})_{\text{B}}$ )	0.77
1605.5 ( $\nu(\text{C}-\text{C})_{\text{S}}$ )	0.67
1226.8 ( $\nu(\text{C}-\text{O}-\text{C})_{\text{S}}$ )	0.73
1240.5 ( $\nu(\text{C}-\text{O}-\text{C})_{\text{B}}$ )	1.47

spectroscopy: (a) 1226.8, (b), (c) 1605.5, (d) 1716.5, and (e) 1240.5  $\text{cm}^{-1}$ . The polar diagrams of 1226.8, 1605.5, and 1716.5  $\text{cm}^{-1}$  exhibit a maximum intensity of absorbance peak along the direction  $90^\circ \longleftrightarrow 270^\circ$  and a minimum intensity along the direction  $0^\circ \longleftrightarrow 180^\circ$ . In addition, the Z-axial component of incident polarized light  $I_z$  achieves the maximum value with an angle of polarization  $90^\circ$  or  $270^\circ$  and the minimum value with an angle of polarization  $0^\circ$  or  $180^\circ$ . Thus, in the PI alignment film, the transition moments  $\nu(\text{C}-\text{O}-\text{C})_{\text{S}}$ ,  $\nu(\text{C}-\text{C})_{\text{S}}$ , and  $\nu(\text{C}=\text{O})_{\text{B}}$  orient parallel to the direction of Z-axial. The polar diagrams of 1240.5 and 1729.0  $\text{cm}^{-1}$  exhibit a maximum intensity of absorbance peak along the direction  $0^\circ \longleftrightarrow 180^\circ$  and a minimum intensity along the direction  $90^\circ \longleftrightarrow 270^\circ$ ,



**Figure 7.** FTIR dichroic spectra of LC cell with pretilt angle being  $2^\circ$ : solid and dashed lines represent the FTIR spectra with IR light polarized perpendicular and parallel to the rubbing direction, respectively.

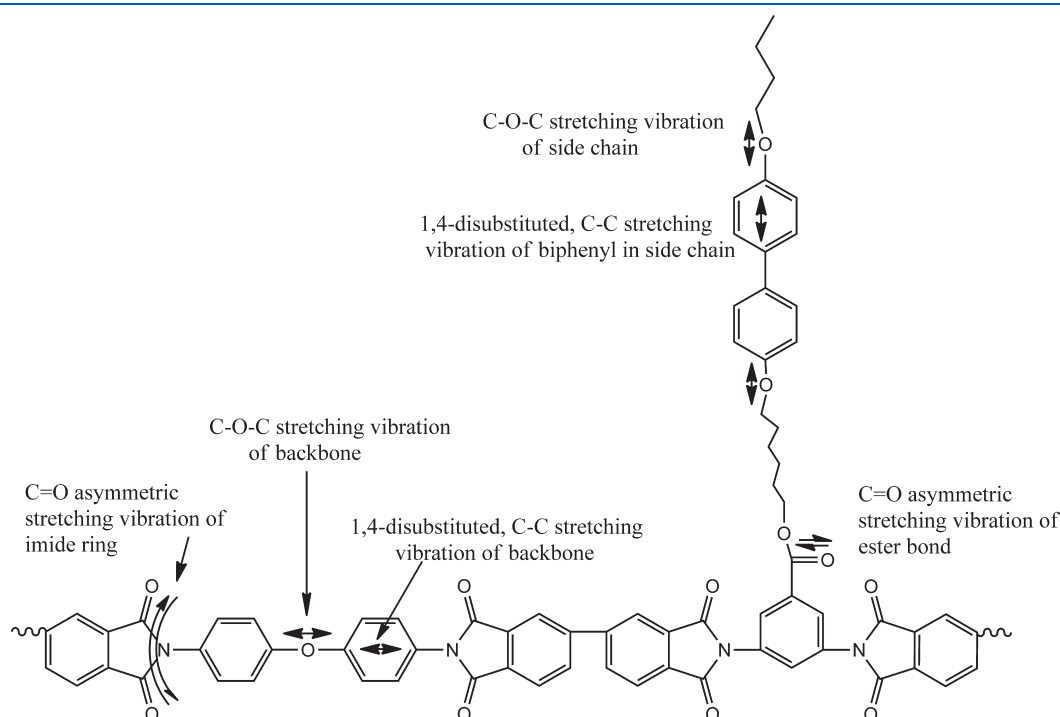


**Figure 6.** Vibration modes and the directions of transition moments for side chained PI molecule.

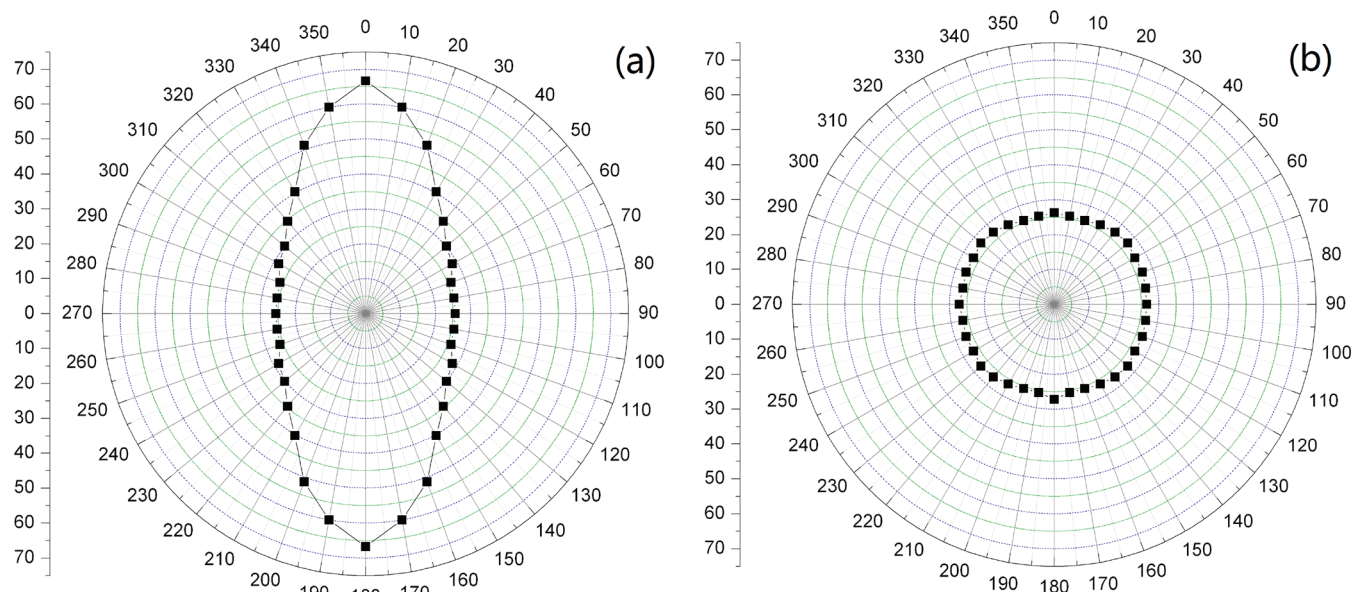


**Figure 8.** Polar diagrams of peaks at  $1602\text{ cm}^{-1}$  of two LC cells with pretilt angle about  $2^\circ$  (a) and  $90^\circ$  (b) as a function of the angle of rotation of the cell.

which indicates that the transition moments  $\nu(\text{C}-\text{O}-\text{C})_{\text{B}}$  and  $\nu(\text{C}=\text{O})_{\text{S}}$  favorably orient parallel to the plane of film.

The position and dichroic ratios for the bands in the spectra under different polarized angle of incident IR beam are listed in Table 3.

As shown in the Figure 6, the averaged directions of transition moments of  $\nu(\text{C}-\text{C})_{\text{S}}$  and  $\nu(\text{C}-\text{O}-\text{C})_{\text{S}}$  are parallel to the para-direction of the biphenyl group in the side chain. Therefore, the dichroic ratios of 0.67 and 0.73 for the  $1605.5\text{ cm}^{-1}$  band of  $\nu(\text{C}-\text{C})_{\text{S}}$  and  $1226.8\text{ cm}^{-1}$  band of  $\nu(\text{C}-\text{O}-\text{C})_{\text{S}}$  indicated that the rigid biphenyl groups in the side chain are oriented in the surface of PI film, with the orientation perpendicular to the surface of PI alignment film. For the molecular backbone, the averaged direction of  $\nu(\text{C}-\text{O}-\text{C})_{\text{B}}$  transition moments is parallel to the long repeat unit axis of molecular backbone and its dichroic ratio is 1.47; it can be confirmed that the PI molecular backbones exhibit higher degrees of in-plane orientation, which mainly resulted from the rigid and planar molecular structures.

The  $\nu(\text{C}=\text{O})_{\text{S}}$  transition moment of ester band joining side chain and molecular backbone is parallel to the long axis and in the repeat plane. It can be seen that it orients parallel to the plane of film because the dichroic ratio is 1.49. In addition, the transition moment of  $\nu(\text{C}=\text{O})_{\text{B}}$  is perpendicular to the long repeat unit axis and in the imide ring plane, and its dichroic ratio is 0.77, which indicates that the imide rings may orient out of plane of the film.

Taken together, it is considered that the rigid biphenyl groups in side chain orient perpendicular to the plane of film surface while the molecular backbones take an in-plane orientation, and the side chains tend to take a perpendicular conformation to molecular backbones. XPS results show that there exists the enrichment of side chains on the film surface. Thus, we consider that the out-of-plane orientation of imide rings may be due to tugging of side chain toward to the surface.

**4.4. The Alignment of LC Analysis by Transmission Polarized FTIR.** Polarized FTIR spectroscopy was used to analyze the alignment orientation of LC molecules in LC cells. In particular, it was investigated whether the para-direction of biphenyl group

in LC molecule oriented perpendicular to the alignment film for the vertical aligned LC cell.

Figure 7 shows representative dichroic IR spectra of one LC cell with pretilt angle  $2^\circ$ . The spectra  $A_{\parallel}$  and  $A_{\perp}$  were obtained with the incident electric field oriented parallel and perpendicular to the selected buffing direction, respectively. The peak at  $1602\text{ cm}^{-1}$  is assigned to the C-C stretching vibration of 1,4- $\text{C}_6\text{H}_4$  of biphenyl group in LC molecules ( $\nu(\text{C}-\text{C})_{\text{L}}$ ). Thus, the dipole transition moments of the  $1602\text{ cm}^{-1}$  orient along the para-direction of the 1,4-disubstituted phenyl ring. The intensity of  $1602\text{ cm}^{-1}$  in spectrum  $A_{\parallel}$  is much weaker than that in  $A_{\perp}$ , which indicates that the biphenyl groups were aligned and the orientation is along the buffing direction. The polar diagrams of peaks at  $1602\text{ cm}^{-1}$  as a function of the angle of rotation of the cell were obtained using linearly polarized IR spectroscopy. As shown in the Figure 8a, the peak is more intense when the polarization of the incident beam is parallel to the rubbing direction for the horizontal aligned LC cell, which further illustrated that the orientation of biphenyl groups is parallel to the buffing direction.

For vertical LC cell, the LC molecules were aligned on the alignment films, so the biphenyl groups of LC molecules should be in order. The polar diagrams of band at  $1602\text{ cm}^{-1}$  for vertical LC cell is shown in the Figure 8b. The peak intensity did not have obvious changes following changing of the angle of rotation. Thus, it can be confirmed that the biphenyl groups were aligned and the para-direction is perpendicular to the alignment film.

Taken together, the polarized FTIR data proved that biphenyl groups in vertical LC cells were aligned orderly and the para-direction oriented perpendicular to the alignment film. In contrast, biphenyl groups in horizontal LC cell oriented parallel to the alignment film and along the buffing direction. In addition, it is the first reported that the alignment of LC molecules and chemical groups in LC cell is investigated by polarized FTIR.

For the main-chain-type polyimide, the chemical groups in the surface generally exhibit higher degrees of in-plane orientation to the plane of alignment film.<sup>28,29</sup> The introduction of side chain always results in the formation of some out-of-plane units on the

surface which can generate high pretilt angle. In our study, the LC molecules on the polyimide (PI—C6BBC4—85) with side chains containing rigid biphenyl groups without buffing process can achieve vertical alignment, and the configuration of molecules in the film surface was investigated by polarized ATR-FTIR. It is found that some chemical groups in the surface, such as biphenyl and imide ring, orient perpendicular to the plane of alignment film while the molecular backbones take the conformation parallel to the plane of film. Because of the similarity of chemical structure and conformation and the enrichment of side chain on the surface, it is much easier for the biphenyl groups of LC molecules to form intermolecular interaction with the biphenyl groups of side chain than with other units on the surface. There exist some intermolecular interactions between LC molecules and biphenyl groups in side chain of polyimide, such as the dipole–dipole and  $\pi$ – $\pi$  interaction, which make it easily to generate a vertical LC alignment on the polymer surfaces.<sup>30</sup> Thus, it is confirmed that the chemical groups in side chains taking a vertical conformation on the surface, such as biphenyl groups, play an essential role in producing a vertical LC alignment.

## 5. CONCLUSIONS

For polyimide with side chain containing rigid biphenyl, the proportion of side chains in the surface of alignment film is obviously higher than that in the bulk. The infrared spectral assignments for this side-chained PI were completed by comparing ATR-FTIR spectra of PI—C6BBC4 with different side chain content. The polarized ATR-FTIR data indicates that some chemical groups, such as biphenyl and imide ring, orient perpendicular to the plane of alignment film while the molecular backbones take the conformation parallel to the plane of film. And, the polarized FTIR data of LC cells indicates that the biphenyl groups of LC molecules in LC cell take the conformation perpendicular to the alignment film. According to the chemical structure and conformation of units on the surface, it is confirmed that the chemical groups in side chains taking a vertical conformation on the surface, such as biphenyl groups, play an essential role in producing a vertical LC alignment.

## AUTHOR INFORMATION

### Corresponding Author

\*Telephone: +86 28 85400377. Fax: +86 28 85405138. E-mail: lxy6912@sina.com.

## ACKNOWLEDGMENT

This work was supported by the National Natural Science Foundation of China (Grants 50773044 and 50973073). We acknowledge Mingbo Yang and the Analytical & Testing Center, Sichuan University, P. R. China, for characterization.

## REFERENCES

- (1) Ghosh, M. K.; Mittal, K. L., Eds. In *Polyimides, fundamentals and applications*; Marcel Dekker: New York, 1996.
- (2) Sroog, C. E. *J. Polym. Sci.: Macromol. Rev.* **1976**, *11*, 161.
- (3) Nishikawa, M. *Polym. Adv. Technol.* **2000**, *11*, 404–412.
- (4) Li, L.; Yin, J.; Sui, Y.; Xu, H. J.; Fang, J. H.; Zhu, Z. K.; Wang, Z. G. *J. Polym. Sci., Part A: Polym. Chem.* **2000**, *38*, 1943.
- (5) Lee, S. B.; Shin, G. J.; Chi, J. H.; Zin, W. C.; Jung, J. C.; Hahn, S. G.; Ree, M. *Polymer* **2006**, *47*, 6606.

- (6) Ichino, T.; Sasaki, S.; Matsuura, T.; Nishi, S. *J. Polym. Sci. Part A: Polym. Chem.* **1990**, *28*, 323.
- (7) Matsuura, T.; Hasuda, Y.; Nishi, S.; Yamada, N. *Macromolecules* **1991**, *24*, 5001.
- (8) Matsuura, T.; Ishizawa, M.; Hasuda, Y.; Nishi, S. *Macromolecules* **1992**, *25*, 3540.
- (9) Cheng, S. Z. D.; Li, F.; Savitski, E. P.; Harris, F. W. *Molecular design of aromatic polyimide films as uniaxial negative birefringent optical compensators in liquid crystal displays*; Elsevier: Cambridge, U.K., 1997.
- (10) Matsumoto, T.; Kurosaki, T. *React. Funct. Polym.* **1996**, *30*, 55.
- (11) Matsumoto, T.; Kurosaki, T. *Macromolecules* **1997**, *30*, 993.
- (12) Matsumoto, T.; Feger, C. *J. Photopolym. Sci. Technol.* **1998**, *11*, 231.
- (13) Volksen, W.; Cha, H. J.; Sanchez, M. I.; Yoon, D. Y. *React. Funct. Polym.* **1996**, *30*, 61.
- (14) Lee, Y. J.; Choi, J. G.; Song, I.; Oh, J. M.; Yi, M. H. *Polymer* **2006**, *47*, 1555.
- (15) Arafune, R.; Sakamoto, K.; Ushioda, S. *Appl. Phys. Lett.* **1997**, *71*, 2755.
- (16) Chern, Y. T.; Ju, M. H. *Macromolecules* **2009**, *42*, 169.
- (17) Lee, Y. J.; Kim, Y. W.; Ha, J. D.; Oh, J. M.; Yi, M. H. *Polym. Adv. Technol.* **2007**, *18*, 226.
- (18) Uchida, T.; Hirano, M.; Sakai, H. *Liq. Cryst.* **1989**, *5*, 1127.
- (19) Sato, Y.; Sato, K.; Uchida, T. *Jpn. J. Appl. Phys.* **1992**, *31*, L579.
- (20) Niwa, M.; Kawakami, H.; Kanamori, T.; Shinbo, T.; Kaito, A.; Nagaoka, S. *Macromolecules* **2001**, *34*, 9039.
- (21) Johnston, C. T.; Premachandra, G. S. *Langmuir* **2001**, *17*, 3712.
- (22) Clark, D. T.; Thomas, H. R. *J. Polym. Sci.: Polym. Chem. Ed.* **1978**, *16*, 791.
- (23) Solomun, T.; Schimanski, A.; Sturm, H.; Illenberger, E. *Macromolecules* **2005**, *38*, 4231.
- (24) Lee, K. W.; Paek, S. H.; Lien, A.; Durning, C.; Fukuro, H. *Macromolecules* **1996**, *29*, 8894.
- (25) Li, L.; Yin, J.; Sui, Y.; Xu, H. J.; Fang, J. H.; Zhu, Z. K. *J. Polym. Sci., Part A: Polym. Chem.* **2000**, *38*, 1943.
- (26) Hatsuo, I.; Stephen, T.; Wellinchoff, E. B.; Jack, L. K. *Macromolecules* **1980**, *13*, 826.
- (27) Chen, H. L.; You, J. W.; Porter, R. S. *J. Polym. Res.* **1996**, *3*, 151.
- (28) Wakita, J. J.; Jin, S. W.; Shin, T. J.; Ree, M. H.; Ando, S. *J. Macromolecules* **2010**, *43*, 1930.
- (29) Ge, J. J.; Li, C. Y.; Xue, G.; Mann, I. K.; Zhang, D.; Wang, S. Y.; Harris, F. W.; Cheng, S. Z. D.; Hong, S. C.; Zhuang, X. W.; Shen, Y. R. *J. Am. Chem. Soc.* **2001**, *123*, 5768.
- (30) Kang, H.; Park, J. S.; Sohn, E. H.; Kang, D.; Rosenblatt, C.; Lee, J. C. *Polymer* **2009**, *50*, 5220.